Journal of Physiology (1989), **412**, *pp.* 197–220
With 10 *text-figures*
Printed in Great Britain

VOLTAGE-DEPENDENT AND CALCIUM-DEPENDENT INACTIVATION OF CALCIUM CHANNEL CURRENT IN IDENTIFIED SNAIL NEURONES

BY M. J. GUTNICK*, H. D. LUX, D. SWANDULLA† AND H. ZUCKER

From the Department of Neurophysiology, Max-Planck-Institute for Psychiatry, Am Klopferspitz 18A, 8033 Planegg-Martinsried, FRG

(*Received 23 May 1988*)

SUMMARY

1. The dependence of Ca^{2+} current inactivation on membrane potential and intracellular Ca^{2+} concentration ($[Ca^{2+}]_i$) was studied in TEA-loaded, identified *Helix* neurones which possess a single population of high-voltage-activated Ca^{2+} channels. During prolonged depolarization, the Ca^{2+} current declined from its peak with two clearly distinct phases. The time course of its decay was readily fitted by a double-exponential function.

2. In double-pulse experiments, the relationship between the magnitude of the Ca^{2+} current and the amount of Ca^{2+} inactivation was not linear, and considerable inactivation was present, even when conditioning pulses were to levels of depolarization so great that Ca^{2+} currents were near zero. Similar results were obtained when external Ca^{2+} was replaced by Ba^{2+}.

3. In double-pulse experiments, hyperpolarization during the interpulse interval served to reprime a portion of the inactivated Ca^{2+} current for subsequent activation. The extent of repriming increased with hyperpolarization, reaching a maximum between -130 and -150 mV. The effectiveness of repriming hyperpolarizations was considerably increased when Ca^{2+} was replaced by Ba^{2+}.

4. A significant fraction of inactivated Ca^{2+} channels can be recovered during hyperpolarizing pulses lasting only milliseconds. If hyperpolarizing pulses were applied before substantial inactivation of Ca^{2+} current, Ca^{2+} channels remained available for activation despite considerable Ca^{2+} entry.

5. The relationship between $[Ca^{2+}]_i$ and inactivation was investigated by quantitatively injecting Ca^{2+}-buffered solutions into the cells. The time course of Ca^{2+} current inactivation was unchanged at free $[Ca^{2+}]$ between 1×10^{-7} and 1×10^{-5} M. From 1×10^{-7} to 1×10^{-9} M, inactivation became progressively slower, mainly due to a decrease of the amplitude ratio (fast/slow) of the two components of inactivation, which fell from about unity to near zero at 1×10^{-9} M. In double-pulse experiments, recovery from inactivation was enhanced in neurones that had been injected with Ca^{2+} chelator.

* Permanent address: Unit of Physiology, Faculty of Health Sciences, Ben Gurion University of the Negev, Beersheva, Israel.

† To whom all correspondence and reprint requests should be addressed.

6. We conclude that inactivation of Ca^{2+} channels in these neurones depends on both $[Ca^{2+}]_i$ and membrane potential. The voltage-dependent process may serve as a mechanism to quickly recover inactivated Ca^{2+} channels during repetitive firing despite considerable Ca^{2+} influx.

7. The results are discussed in the framework of a model which is based on two states of inactivation, IN_V and IN_{Ca}, which represent different conformations of the inactivating substrate, and which are both reached from a lumped state of activation (A). Inactivation leads to high occupancy of IN_V during depolarization. Transitions from IN_V to A as well as to IN_{Ca} are considered to depend on voltage. Ca^{2+} dependence is attributed to the two transition rates leading to IN_{Ca}. Fast repriming kinetics are expressed by a significant increase of the voltage- and Ca^{2+}-dependent rate leading from IN_V to IN_{Ca}. Intermediate high occupancy of state IN_{Ca} is subsequently discharged into state A.

INTRODUCTION

In voltage-clamped molluscan neurones, as in other preparations, calcium currents evoked by a prolonged depolarizing pulse gradually decline from an initial peak due to a process of Ca^{2+} channel inactivation (for review see Kostyuk, 1980; Hagiwara & Byerly, 1981; Tsien, 1983). There is a considerable body of evidence which indicates that inactivation of macroscopic Ca^{2+} currents is sensitive to the intracellular concentration of Ca^{2+} ($[Ca^{2+}]_i$) (Brehm & Eckert, 1978; Tillotson, 1979; Brehm, Eckert & Tillotson, 1980; Ashcroft & Stanfield, 1981; Plant & Standen, 1981). This has led to the assertion that Ca^{2+} inactivation in molluscan neurones is a Ca^{2+}-mediated process (Eckert & Tillotson, 1981; Plant & Standen, 1981; Eckert & Ewald, 1983; Plant, Standen & Ward, 1983; Eckert & Chad, 1984; Chad & Eckert, 1986). However, Brown, Morimoto, Tsuda & Wilson (1981) concluded that in snail neurones, the mechanism of inactivation entails both voltage-dependent and Ca^{2+}-dependent components (see also Yatani, Wilson & Brown, 1983; Lux & Gutnick, 1986). Other authors have reached similar conclusions for other preparations (Kass & Sanguinetti, 1984; Lee, Marban & Tsien, 1985; Hadley & Hume, 1987; Akaike, Tsuda & Oyama, 1988; Argibay, Fischmeister & Hartzell, 1988).

Studies of the behaviour of single Ca^{2+} channels in identified snail neurones demonstrated that inactivation of macroscopic Ca^{2+} current is associated with a decrease in the probability of channel opening with time. Lux & Brown (1984*a*) showed that inactivation of single-channel currents is not strongly related to prior Ca^{2+} entry through the channels. Thus pre-existing intracellular levels of Ca^{2+} may be sufficient to mediate Ca^{2+}-dependent inactivation.

In the experiments reported here, we have quantitatively evaluated the relationship between $[Ca^{2+}]_i$ and Ca^{2+} inactivation in identified neurones of the land snail, *Helix pomatia*. We have also examined the effect of membrane potential and $[Ca^{2+}]_i$ on recovery from inactivation. Our results are considered in the framework of a specific, two-inactivation-state model which describes the way in which $[Ca^{2+}]_i$ and membrane potential interact to regulate the availability of Ca^{2+} channels. A preliminary report of this work has appeared (Swandulla, Lux, Gutnick & Zucker, 1988).

METHODS

Preparation and recording

The neuronal cell bodies of U cells (100–150 μm diameter) used in this study form a cluster in the right parietal ganglion of *Helix pomatia*. After removing the connective tissue, which was exposed to 1% pronase for 5 min, the cell bodies were isolated by axotomy about 500 μm from the soma (Lux & Hofmeier, 1982). The bathing solution was sodium-free and contained (in mM): $CaCl_2$, 40; $MgCl_2$, 5; KCl, 4; tetraethylammonium (TEA)-Cl, 45; 4-aminopyridine (4-AP), 5; glucose, 5 and HEPES, 5 (pH 7·8). For Ba^{2+}studies, Ba^{2+} was substituted isosmotically for Ca^{2+}. Experiments were done at a bath temperature of 20 °C, unless otherwise noted. Temperature was held within 0·2 °C with a thermo-electric device having a thermistor in a feed-back configuration.

Techniques for voltage clamp with two intracellular electrodes were as previously described by Hofmeier & Lux (1981). The membrane potential was measured differentially between an intracellular microelectrode filled with 3 M-KCl and a KCl–agar extracellular electrode positioned near the ganglion. The series resistance was measured to be about 15 kΩ. The largest recorded currents of 0·2 μA were expected to produce a voltage offset of 4 mV or less. For this reason, the series resistance was only partially compensated. A current-to-voltage circuit, which provided a virtual ground, was used to collect whole-cell current. Current was delivered by a microelectrode of 0·5–1·5 MΩ filled with a mixture of 3 M-CsCl and 1 M-TEA-Cl. To minimize interaction with the voltage-recording electrode, the current electrode was shielded to the tip by an electrically grounded silver coat. The silver was applied by immersing the capillary tip into an organic silver chelate (Lapidol II; Doduko Co., Rockford, IL, USA) and by subsequent annealing with heat, as described by Lux & Hofmeier (1982). The plated electrodes were then repeatedly dipped into a varnish and thereby insulated from the bath. Unless otherwise stated, the holding potential was −50 mV. Currents were measured and stored on FM tape for subsequent digitization and computer analysis. Compensation for symmetrical leakage and capacitive currents was accomplished by subtracting current responses to hyperpolarizing pulses of the same magnitude from currents evoked by depolarizing pulses.

The TEA-Cl in the bathing medium and in the current electrodes served to suppress K^+ currents. The 1 M-TEA-Cl stock solution was extracted with ethylether to remove any contaminating triethylamine that might alkalize the cell (Zucker, 1981). 4-AP was also used as a K^+ blocker.

Buffer solutions were injected into the cells using a fast, quantitative method of pressure injection which is described in detail by Hofmeier & Lux (1981). Injection electrodes were pulled in two steps. In the first step the capillary was evenly thinned over a length of about 15 mm to provide a cylindrical solution chamber with an inner diameter of 30–50 μm. In the second step the tip, with a diameter of 1–2μm, was formed. Potassium ion exchanger was injected from the back into the solution chamber before injection solution was sucked through the tip. The ion exchanger formed a phase boundary with the injection solution which was easily visible under the microscope. The injected quantity was estimated with a resolution of 10^{-11} l from the shift of the phase boundary measured with an ocular micrometer. The use of the ion exchanger allowed recording of the membrane potential, which indicated the intracellular location of the electrode tip.

Internal buffering with calcium chelators

Ca^{2+} buffers

For intracellular pressure injection of Ca^{2+} buffers, a third electrode was introduced, which contained in addition 50 mM-proton buffer (HEPES or Tris, adjusted to pH 7·25 with CsOH) and in some experiments 35 mM-TEA-Cl. 100 mM-EGTA (ethyleneglycol-bis-(β-aminoethylether)-*N,N,N',N*-tetraacetic acid) or 50 mM-BAPTA (bis(*o*-aminophenoxy)ethane-*N,N,N',N*-tetraacetic acid, dried at 150 °C) were used as the chelators for Ca^{2+} buffers with free $[Ca^{2+}]$ levels $< 5 \times 10^{-6}$ M, which were calculated with an apparent stability constant of $9{\cdot}6 \times 10^6$ M^{-1} (Harafuji & Ogawa, 1980) for EGTA and $9{\cdot}33 \times 10^6$ M^{-1} (Tsien, 1980) for BAPTA.

100 mM-HEDTA (*N*-(2-hydroxyethyl)ethylenedinitrilo-*N,N',N'*-triacetic acid), stability constant $4{\cdot}3 \times 10^5$ M^{-1} (Martell & Smith, 1974), was used to buffer free $[Ca^{2+}]$ at levels $> 5 \times 10^{-6}$ M.

For the pH-sensitive EGTA–Ca^{2+} buffers, pH changes related to increases in $[Ca^{2+}]_i$ at the inner channel mouth during channel opening (see Fig. 1) were estimated to be not more than 0·2 pH units. The EGTA was from Merck, the BAPTA from Fluka and the HEDTA from Sigma.

Spatio-temporal Ca^{2+} buffering

Based on single-channel current measurements in *Helix pomatia* neurones and data on cytoplasmic buffering in *Aplysia* neurones, Chad & Eckert (1984) calculated steady-state increases in free $[Ca^{2+}]_i$ in a hemisphere (domains) of 50 nm radius surrounding the inner mouth of a Ca^{2+} channel of about 1×10^{-5} M for maximum Ca^{2+} current activated at 0 mV. Such a concentration would be efficiently buffered by adding large amounts of high-affinity Ca^{2+} chelators to the cellular buffers as was done in our experiments. It was noted by Neher (1986) that the introduction of the

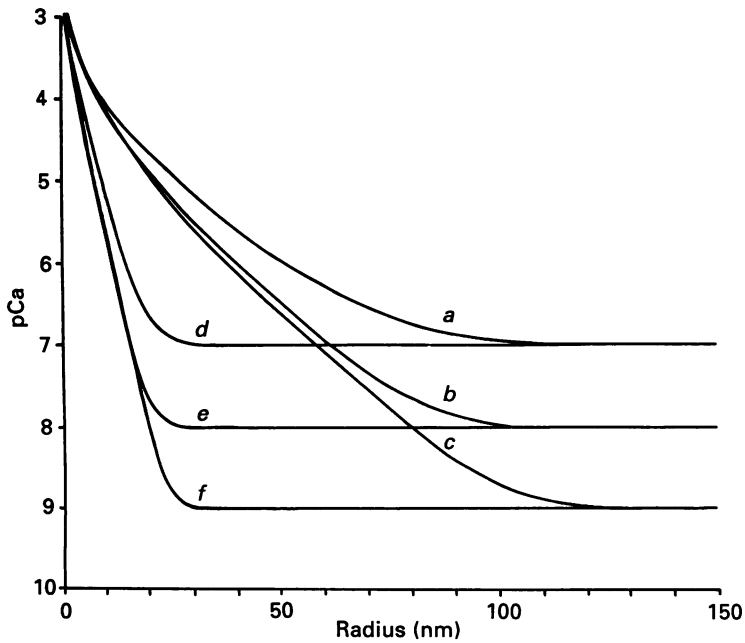

Fig. 1. Spatial profile of Ca^{2+} concentration (pCa, negative logarithm of free $[Ca^{2+}]$) during Ca^{2+} influx in the surround of the inner channel mouth in the presence of EGTA–Ca^{2+} (a, b, c) and BAPTA–Ca^{2+} buffers (d, e, f). Free Ca^{2+} concentrations set by the buffers are 1×10^{-7} M (a, d), 1×10^{-8} M (b, e) and 1×10^{-9} M (c, f). Total chelator concentration is 100 mM for EGTA and 50 mM for BAPTA. Curves are generated applying the approach of Crank (1956) and Neher (1986) for Ca^{2+} chelation as determined by radial Ca^{2+} diffusion from a point source and reaction times of buffers. For a point source in a half-space, $[Ca^{2+}]_r = i(4\pi FDr)^{-1} \exp(-r/\theta)$, with $[Ca^{2+}]_r$ = increase in Ca^{2+} concentration at the radial distance r within the plane of the membrane; i = single-channel current (0·4 pA, Lux & Brown, 1984*b*); F = Faraday constant; D = diffusion constant (2×10^{-6} cm^2 s^{-1}); $\theta = (\frac{1}{2} Dk^{-1}[L]^{-1})^{\frac{1}{2}}$, thickness of the disc in which Ca^{2+} chelation takes place; k = association rate of the chelation (EGTA, $9{\cdot}6 \times 10^6$ M^{-1} s^{-1}; BAPTA, $4{\cdot}3 \times 10^8$ M^{-1}s^{-1}); [L] = concentration of free chelator. Concentration values are reached within microseconds with a time constant of $\tau = k^{-1}[L]^{-1}$.

finite reaction time of the buffer results in an expansion of the volume in which complexation takes place. Thus, in our calculations, Ca^{2+} ions are allowed to diffuse away from the inner channel mouth before they are chelated. The spatio-temporal profile of buffering is primarily determined by the association rate of the Ca^{2+}–chelator complex in addition to the concentration of free chelator. For BAPTA, the apparent association rate of the complex is $4{\cdot}3 \times 10^8$ M^{-1} s^{-1} (value taken for Quin-2, see Quast, Labhardt & Doyle, 1984), which is about two orders of magnitude larger than that of EGTA ($9{\cdot}6 \times 10^6$ M^{-1} s^{-1}, see Harafuji & Ogawa, 1980). Figure 1 shows the radial Ca^{2+} concentration profiles in the membrane area around a point-source of Ca^{2+} entry, which represents the inner channel mouth, in the presence of various EGTA- (a, b, c) and BAPTA–Ca^{2+} buffers (d, e, f). Due to

the fast on-rates of the buffer systems, steady-state concentration levels are reached in less than 10 μs (Fig. 1, see also Neher, 1986). The calculations use a diffusion coefficient $\frac{1}{3}$ of that in water (Connor & Nikolakopoulou, 1982). These [Ca^{2+}] profiles are steep enough to restrict increases in free $[Ca^{2+}]_i$ to single channels as can be inferred from typical channel densities. Single-channel density for the visible cell surface was estimated to be 3 μm^{-2} in our preparation, but was determined to be less ($\leqslant 1$ μm^{-2}) by capacitance measurements which take into account the entire membrane area including infoldings (Lux & Brown, 1984*b*, and unpublished observations). Membrane patches of 2–20 μm^2 as obtained with small (diameter $\leqslant 1$ μm) pipette tips contained up to fifty channels with a mean of about four channels, with no evidence for channel densities higher than 10 μm^{-2}. Comparing data on membrane area and averaged single-channel Ca^{2+} currents with currents delivered by macroscopic membrane patches, similar low channel densities (0·1–0·7 μm^{-2}) can be derived from data on other molluscan neurones. Even patches reported to show an unusually high current density ('hot spots') contain on average probably not more than one channel per μm^2 (see Thompson & Coombs, 1988). Assuming 'hot spots' with an average of ten channels per μm^2 in our preparation, the mean distance between channels would be about 300 nm. Even in this case individual channels would be sufficiently isolated in the presence of the injected buffers. Realistically, the whole-cell current is expected to flow in its majority through channels distributed at a lower density in the membrane.

Exponential curve fitting

Inactivation kinetics were fitted with the double-exponential function:

$$-I(t) = a + b\exp(-\lambda_1 t) + c\exp(-\lambda_2 t), \qquad (\alpha)$$

where $I(t)$ is the inactivating current as a function of time, a is the current amplitude at $t = \infty$, b and c are the amplitudes of the time-dependent components and λ_1 and λ_2 are the reciprocals of the fast (τ_f) and the slow (τ_s) time constant of inactivation respectively. The five parameters in the equation were determined by a least-squares fitting routine described by Marquardt (1963).

RESULTS

Calcium channel currents

It has been shown that Ca^{2+} current is the predominant inward current, and Ca^{2+}-dependent K^+ current the principle outward current in the neurones investigated (Lux & Hofmeier, 1982). Thus, inward currents showed little if any change when, in the bathing medium, Na^+ was replaced by Tris or choline, nor were they affected by addition of tetrodotoxin (TTX, 5×10^{-4} M). The solutions used in the experiments were designed to isolate the membrane currents through Ca^{2+} channels. The combined use of tetraethylammonium (TEA) and 4-aminopyridine (4-AP) successfully suppressed K^+ outward currents (see also Brown *et al.* 1981; Plant & Standen, 1981), as indicated by the finding that even with a depolarizing step from -50 mV to $+100$ mV, the magnitude of the time-dependent outward current was only one-tenth that of the peak inward current at $+30$ mV. Figure 2 shows the voltage-dependent inward currents carried by Ca^{2+} or Ba^{2+} recorded under these experimental conditions. Ca^{2+} channel currents were completely abolished when channel blockers such as cadmium (100 μM) were added to the medium or when Ca^{2+} was replaced by magnesium or nickel.

Even with hyperpolarization as negative as -120 mV, there was no evidence in this preparation for other, low-voltage-activated Ca^{2+} currents, as were recently identified in a variety of other excitable tissues (see e.g. Carbone & Lux, 1984; Deitmer, 1984; Armstrong & Matteson, 1985; Bean, 1985; Bossu, Feltz & Thomann, 1985; Fedulova, Kostyuk & Veselovsky, 1985; Nowycky, Fox & Tsien, 1985). Also, there was no indication of a second peak in the current–voltage curve of these neurones,

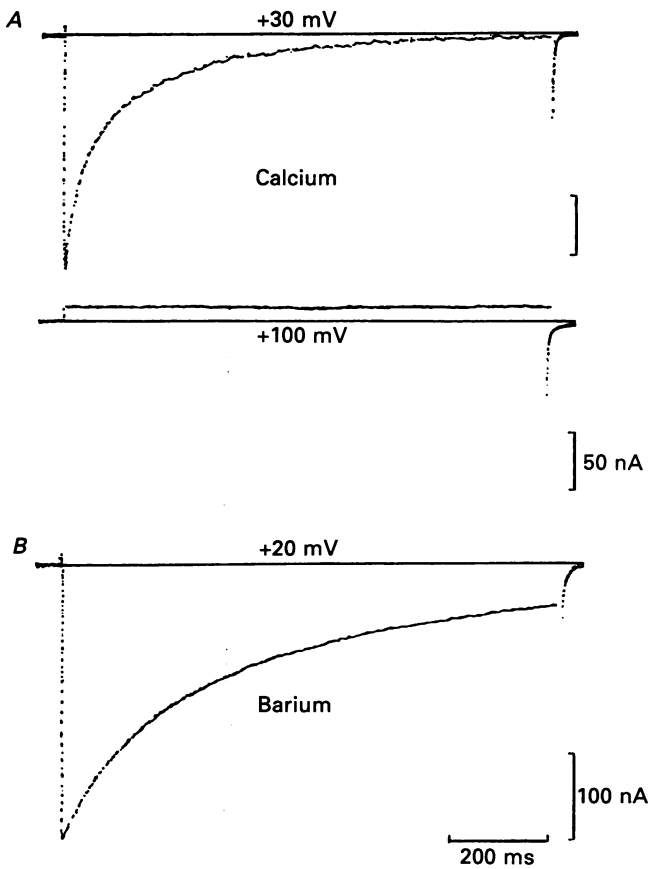

Fig. 2. Inactivation of Ca^{2+} channel current. Current signals were recorded from a TEA-loaded neurone during depolarizing pulses from a holding potential of −50 mV to the potentials indicated, in the presence of 40 mM-Ca^{2+} (*A*) and 10 min after substituting Ba^{2+} for Ca^{2+} isosmotically (*B*). In these and subsequent recordings linear components of leakage and capacitance were removed by subtraction of currents obtained with hyperpolarizing pulses of the same magnitude. Temperature 30 °C.

and tail currents measured 0·3 ms following the activating pulse showed one fast decaying component that was well fitted by a single exponential.

Characteristics of inactivation

Ca^{2+} inactivation was evident as decay from the peak of the inward current during depolarizing steps, and as a decrease in the peak Ca^{2+} current during the second of a pair of depolarizing pulses. As has previously been reported (Kostyuk & Krishtal, 1977; Brown *et al.* 1981), inward current during a sustained depolarization showed an initial, rapid relaxation from the peak, followed by a more gradual decay. The turn-off process was, within 1 s, always well approximated by a double-exponential expression with the two time constants τ_f and τ_s (for details see Methods). At 30 °C, and with pulses to +30 mV, τ_f and τ_s were 27·5 ± 9 and 240 ± 50 ms, respectively. The amplitude ratio b/c, from eqn (α), of the fast and slow component of inactivation was 1·1 ± 0·2 ($n = 21$) at time zero. The extent of inactivation was also manifested by a

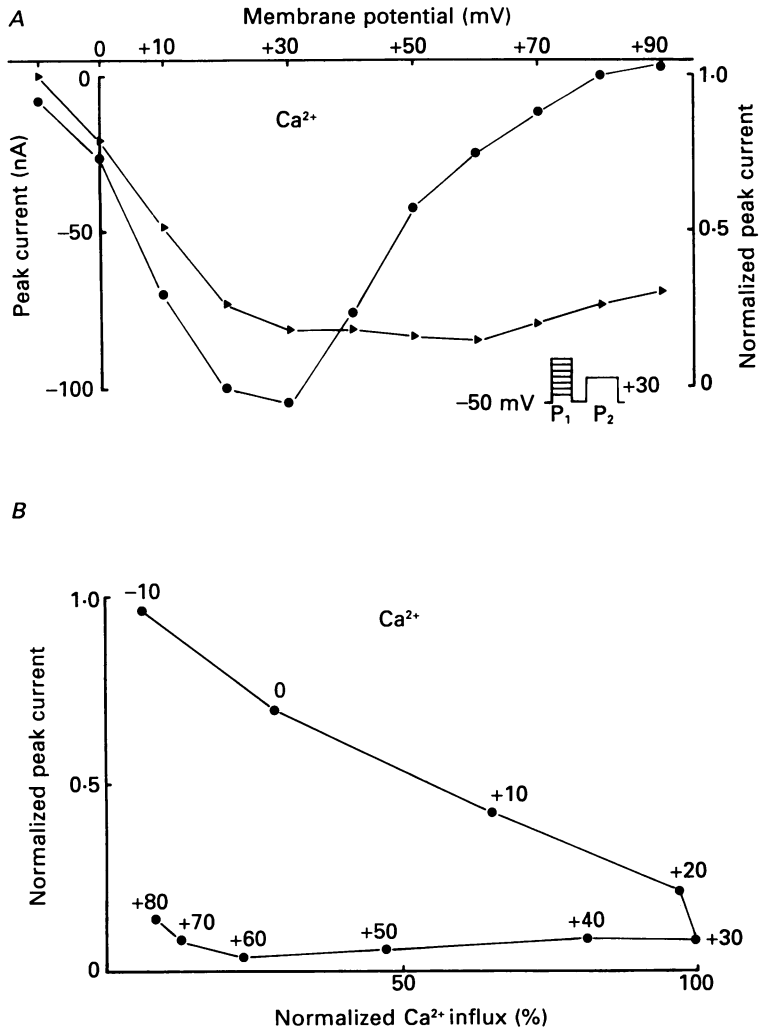

Fig. 3. *A*, *I–V* relationship for Ca^{2+} channel current in 40 mM-Ca^{2+} solution (●). Depolarizing pulses (400 ms) were from a holding potential of −50 mV. Recovery from inactivation as a function of pre-pulse amplitude (▲). Pre-pulses (P_1) (60 ms) to different depolarizing membrane potentials were followed by test pulses (P_2) to +30 mV after 10 ms of repolarization to −50 mV (see inset). The peak currents of the test pulses were normalized to the peak current of an unconditioned test pulse and plotted against voltage. *B*, relationship between normalized peak current and normalized Ca^{2+} influx during the test pulse. Current–time integrals of the test pulses were normalized to that of an unconditioned test pulse. Membrane potential of each pre-pulse is shown in millivolts with each data point. Temperature 30 °C.

decrease in the amplitude of the inward tail currents measured upon repolarization following activating pulses of various duration (see also Brown *et al.* 1981; Eckert & Tillotson, 1981). Lowering the temperature slowed the time constants and reduced the peak inward current with a Q_{10} (temperature coefficient) near 2 between 36 and 8 °C. However, there was no gross, qualitative difference between the results of experiments performed at various temperatures in this range.

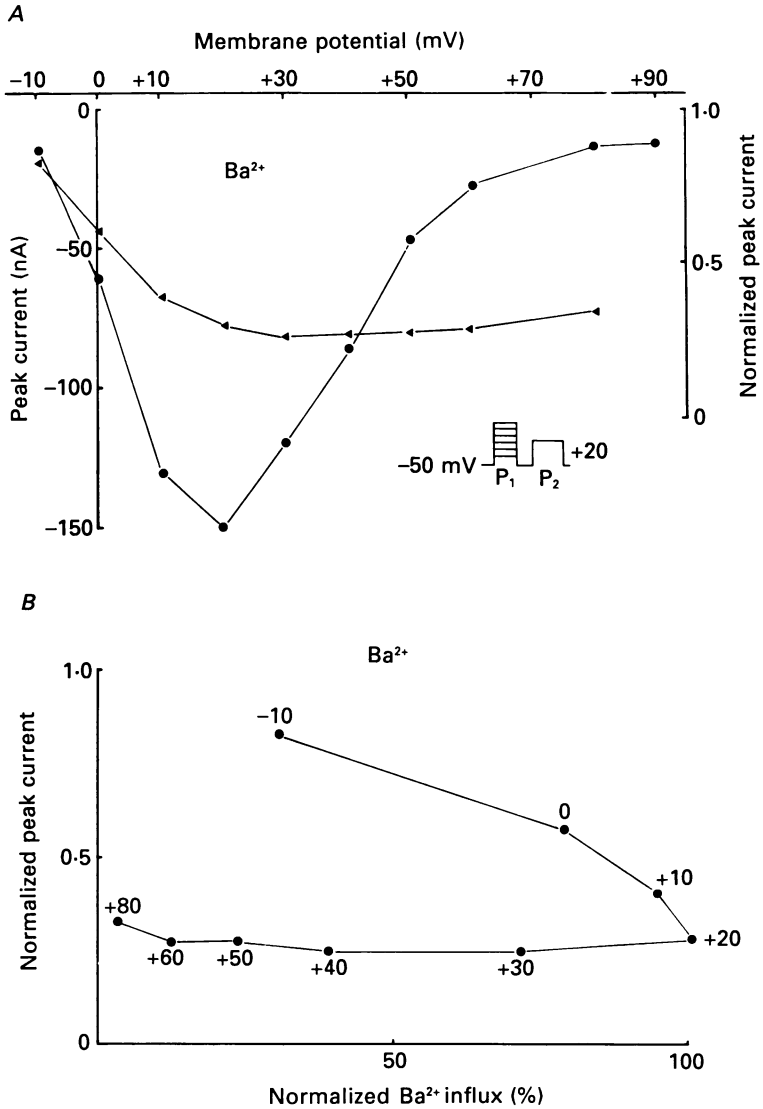

Fig. 4. Same plots as in Fig. 3 for Ca^{2+} channel currents in 40 mM-Ba^{2+} solution. Pre-pulses were 260 ms in duration. Test pulses were to +20 mV. Temperature 30 °C.

Effects of substituting barium for calcium

As has previously been reported (Magura, 1977; Connor, 1979; Adams & Gage, 1980; Brown *et al.* 1981), replacement of Ca^{2+} with Ba^{2+} resulted in larger inward currents, a shift to the left of the I–V curve by about 10 mV, and slowing of inactivation (Fig. 2*B*). The slow relaxation of the Ba^{2+} current did not reflect an inability of Ba^{2+} to activate outward K^+ currents, since, as shown in Fig. 2*A*, these currents were negligible in our experiments. The time course of inactivation in Ba^{2+} in most experiments was best fitted by a single-exponential expression.

Effects of conditioning pre-pulses on calcium and barium currents

The hypothesis that Ca^{2+} inactivation is Ca^{2+}-dependent was initially based on results of double-pulse experiments in which pre-pulse voltage was systematically varied and the effect on peak current during a subsequent rest pulse was measured. Several authors reported that Ca^{2+} inactivation first increases and then decreases as a function of depolarization, resulting in a U-shaped inactivation curve to reflect a quantitative dependence on Ca^{2+} entry during the pre-pulse rather than on voltage (for review see Eckert & Chad, 1984). We tested for this behaviour using rather short (4–20 ms) compared to the previously reported long (100–400 ms) interpulse intervals to prevent substantial recovery from inactivation between activating pulses. We found that under these conditions inactivation was only weakly dependent on prior Ca^{2+} entry. This is illustrated in Fig. 3*A*, which shows the effect of varying the potential of a 60 ms pre-pulse on the Ca^{2+} current evoked 10 ms later by a test pulse to +30 mV. The amount of inactivation increased steadily to a maximum at +60 mV, and then fell off slightly as the depolarization increased further (see also Brown *et al.* 1981). Thus, inactivation was still substantial at +90 mV even though Ca^{2+} current was near zero at this high level of depolarization. The lack of correlation between Ca^{2+} inactivation and Ca^{2+} entry is further illustrated in Fig. 3*B*, which shows a plot of the peak current during the test pulse against the preceding Ca^{2+} influx which was obtained from the current–time integral of both the pre-pulse current and the tail current recorded on repolarization to −50 mV between activating pulses. Tail currents decayed with a time constant of less than 1 ms at this potential, and thus channels at the end of the interpulse interval should be either available for activation or inactivated. This assumption was supported by the finding that currents during the pre-pulse as well as during the test pulse activated with a similarly fast time course, even with interpulse intervals as brief as 4 ms. Figure 4 shows that substitution of Ba^{2+} for Ca^{2+} results in the same qualitative relationships between peak current, cation entry and inactivation. However, in these experiments, the conditioning pulses were prolonged to 260 ms to compensate for the slower time course of inactivation with Ba^{2+} as the charge carrier. Although there is no simple relationship between influx of divalent cations and amount of inactivation, Ca^{2+} ions do affect the development of the inactivation process, as shown below.

Voltage dependence of recovery from inactivation

One indication of the voltage dependence of the Ca^{2+} inactivation process was the finding that the recovery of inactivated channels (repriming) was sensitive to membrane potential. The repriming effect of even brief hyperpolarization could be demonstrated with a repetitive pulse protocol, as illustrated in Fig. 5*A*. In this figure, the current generated during a prolonged depolarizing step to +30 mV is superimposed on that generated by a train of depolarizing pulses interrupted by 4 ms intervals to −110 mV. It can be seen that the pulse train was associated with substantially less inactivation even though it evoked about twice as much Ca^{2+} entry (as inferred from the time integral of the current including the tails). It is thus evident that the hyperpolarizing pulses accelerated recovery of inactivated channels, and that inactivation was not a consequence of the Ca^{2+} entry alone. We used a

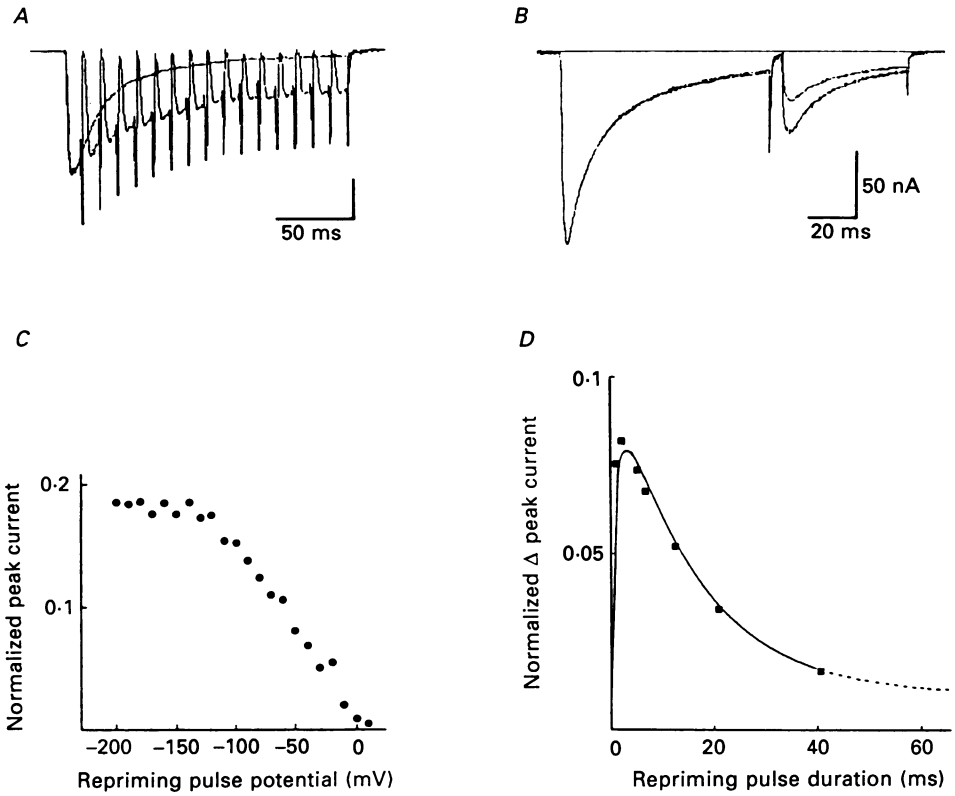

Fig. 5. Voltage-dependent repriming of inactivated Ca^{2+} current. *A*, current generated during a prolonged depolarizing step from −50 to +30 mV was superimposed on current generated during a train of depolarizing pulses interrupted by 4 ms intervals of hyperpolarization to −110 mV. Temperature 18 °C. *B*, superimposed are two current recordings obtained with double pulses to +30 mV. Pre-pulses were from −50 mV, and test pulses from −50 (upper trace) and −125 mV (lower trace), respectively. Interpulse interval was 5 ms. Note that tail currents do not contribute significantly to the Ca^{2+} influx during the pre-pulses. *C*, similar experiment to that in *B* with repriming pulses to a variety of membrane potentials. Peak current during the second of the pair of depolarizing pulses is normalized to peak current during the pre-pulse and plotted against membrane potential reached during the interpulse interval. *D*, time dependence of hyperpolarizing repriming. Similar experiment to that in *B* with repriming pulses of varied duration to −50 and −100 mV, respectively. Peak current during the second of the pair of depolarizing pulses is normalized to peak current during the pre-pulse. The difference between normalized peak currents (normalized Δ peak current) for −100 and −50 mV was plotted against duration of repriming. Note that the added repriming effect of increased hyperpolarization decreases as repriming pulse duration increases. The data points are well approximated (continuous line) by assuming that additional repriming is mainly due to a smaller time constant (2·5 ms) of the recovery process at −100 than at −50 mV (16 ms). For longer-lasting (>40 ms, dashed line) repriming pulses slower time constants become effective (for details see Discussion) which were not considered in this experiment. Temperature 20 °C.

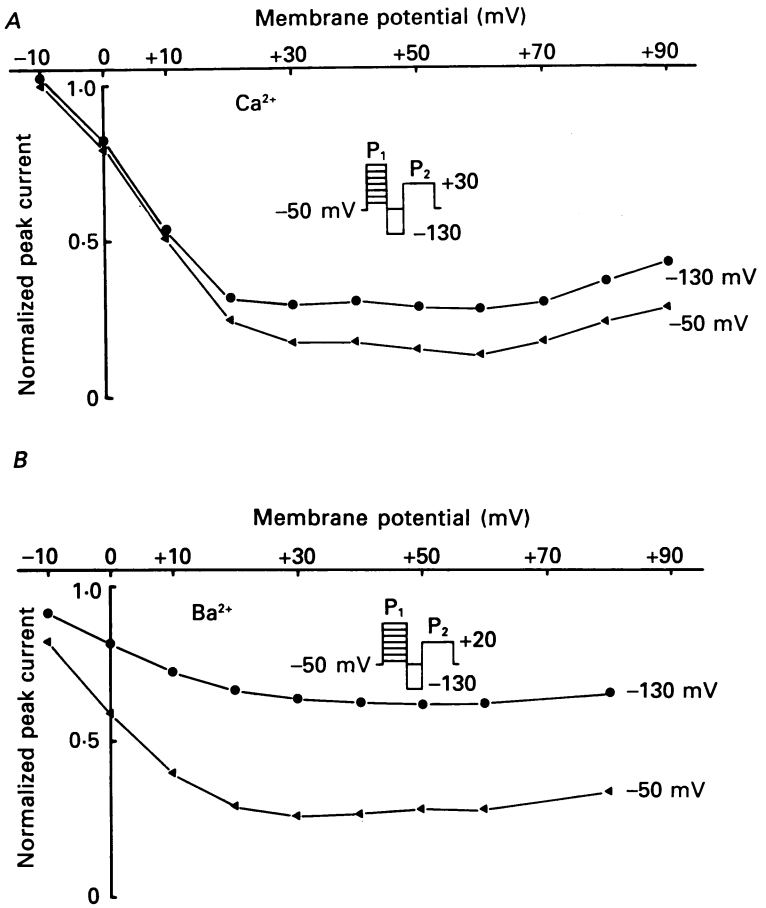

Fig. 6. *A*, voltage-dependent recovery from inactivation as a function of pre-pulse amplitude. Pulse protocol was as shown in the inset. 60 ms pre-pulses (P_1) to a variety of depolarizing membrane potentials were followed by 1 s test pulses (P_2) to +30 mV after the membrane was repolarized for 10 ms to −50 (▲) and −130 mV (●), respectively. P_2 was normalized to the peak current of an unconditioned test pulse and plotted against voltage. *B*, same plots as in *A*, with Ba^{2+} substituting for Ca^{2+} in the external solution. Pre-pulses were 260 ms duration, and test pulses were to +20 mV (see inset). Temperature 20 °C.

double-pulse protocol to examine the dependence of recovery from inactivation on the repriming pulse potential and duration. Large hyperpolarizing pre-pulses had no effect when they preceded unconditioned depolarizations. However, hyperpolarizing the membrane during the interpulse interval served to enhance reactivation of inactivated Ca^{2+} channels. This is illustrated in Fig. 5*B*, which shows that the current during the second of a pair of activating pulses was larger in amplitude when repolarizing the membrane between pulses to −125 mV instead of the usual holding potential of −50 mV. The amount of repriming was a direct function of membrane potential for voltages less negative than −130 mV; further hyperpolarization caused no further repriming (Fig. 5*C*). The data of Fig. 5*B* were obtained with an interpulse

interval of 5 ms. As the duration of this interval increased, and inward current recovered, hyperpolarization became less effective (see also Fig. 9*A*). The enhancement of repriming conferred by an additional 50 mV of hyperpolarization strongly decreased within tens of milliseconds (Fig. 5*D*). This could explain why decreased inactivation following interpulse hyperpolarization was not seen in previous studies which examined interpulse intervals of long (200 ms) duration (Eckert & Tillotson, 1981).

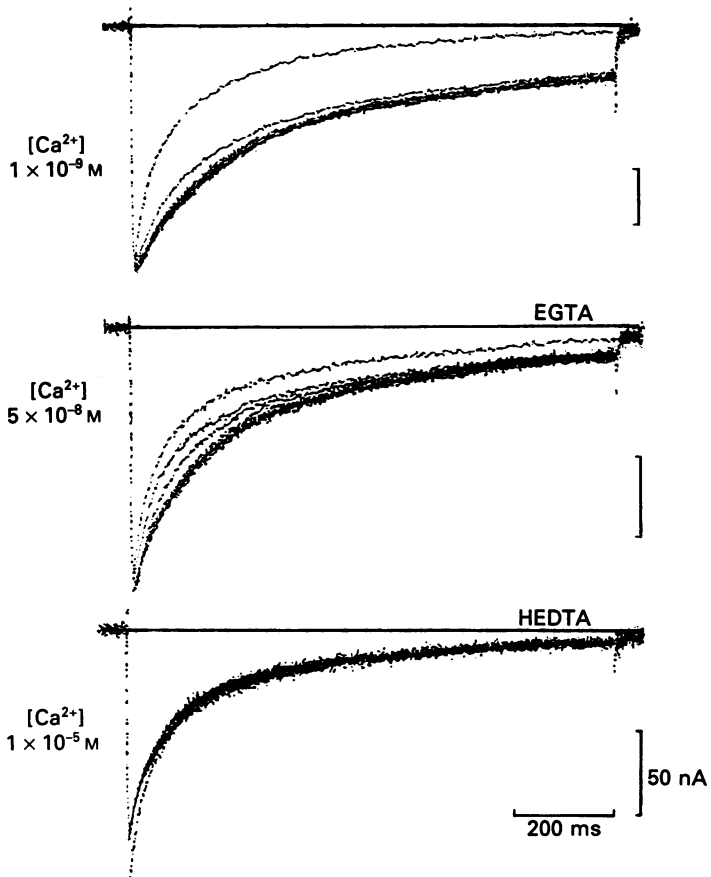

Fig. 7. Effect of internal buffering on Ca^{2+} current inactivation. Cells were injected with EGTA–Ca^{2+} or HEDTA–Ca^{2+} buffers. Free [Ca^{2+}] of the buffers was as indicated. Ca^{2+} current inactivation was slowed with subsequent injections (upper and middle traces). The effect became saturated with internal buffer concentrations of about 30 mM (for details see text). Ca^{2+} current inactivation was minimally affected with free [Ca^{2+}] levels above 10^{-7} M (lower trace), although slight reductions in peak current were observed at these concentrations. Temperature 20 °C.

Nevertheless, evidence was obtained which indicated that intracellular Ca^{2+} does affect the repriming process. Once largely inactivated, relatively little of the Ca^{2+} current could be restored by hyperpolarizing pulses. This is illustrated in Fig. 6*A*, which plots the relationship between voltage and inactivation as measured with a double-pulse protocol, and shows that repriming was enhanced by not more than

15% when the membrane potential was stepped to −130 mV rather than −50 mV during the interpulse interval. Figure 6*B* shows that when Ca^{2+} was replaced by Ba^{2+}, hyperpolarization during the interpulse interval was about twice as effective.

Taken together, these data suggest that Ca^{2+} entry does interfere in some way with the voltage-dependent repriming process. In order to clarify the role of Ca^{2+}, we next undertook a direct examination of the relationship between $[Ca^{2+}]_i$ and the parameters of Ca^{2+} inactivation.

Quantitative intracellular injection of buffered calcium

Quantitative intracellular injections of buffered Ca^{2+} were made in order to directly determine the relationship between free $[Ca^{2+}]_i$ and the inactivation process. Average cell volume, as determined from measurements of the largest and smallest soma diameters to account for deviations from a spherical shape, was 1 nl. Intracellular injections were done in steps of 100–200 pl. Thus, each step raised the intracellular Ca^{2+} buffer concentration by about 10–20 mM. Cell size returned to normal within minutes after the injections. Ten to twenty injections were made over 15–30 min. Cells were discarded if a leakage current >0·5 nA appeared with the injections.

Effectiveness of intracellular Ca^{2+} buffering

When the solution in the injection pipette had a free $[Ca^{2+}]$ level of 1×10^{-8} M or below, the first injection was usually sufficient to produce a detectable increase in the slow phase of decay of the Ca^{2+} current (Fig. 7). This effect became progressively more pronounced with subsequent injections, until the intracellular concentration of Ca^{2+} buffer reached about 30 mM, at which point the effect became saturated and additional injections did not produce further change in the time course of the current decay. Since addition of still more buffer had no obvious deleterious effect on cell viability, injection of each cell was continued. Calculated final concentrations of total chelator were between 60 and 130 mM.

Relationship between inactivation and free $[Ca^{2+}]$ set by the buffer

As may be seen in Fig. 7, Ca^{2+} currents in cells buffered at concentrations between 1×10^{-5} and 5×10^{-8} M were similar in appearance to those of uninjected cells. Buffering free $[Ca^{2+}]$ levels lower than 5×10^{-7} M had little or no effect on the peak amplitude of the Ca^{2+} current. At higher concentrations, the current was always somewhat reduced. This finding is similar to that reported by Plant *et al.* (1983) on the effects of injecting about 11 mM-EGTA. The extent of the current reduction varied considerably from cell to cell and in some cases was very small, despite high $[Ca^{2+}]$ levels. Thus, the reduction was less than 20% in several cells at 10^{-6} M, and in one cell at 10^{-5} M (Fig. 7). The most profound effect of buffer injection was on the time course of the inactivation, as is shown in Fig. 8. Fitting double exponentials to the decay of the inward current revealed that the fast time constant increased somewhat with decreasing free $[Ca^{2+}]$, while the slow time constant was almost unaffected. However, the relative contributions of the fast and slow component of the decay, as expressed by the ratio of their amplitudes, was markedly affected. This ratio fell steadily as free $[Ca^{2+}]$ decreased below 1×10^{-7} M, and at 1×10^{-9} M the

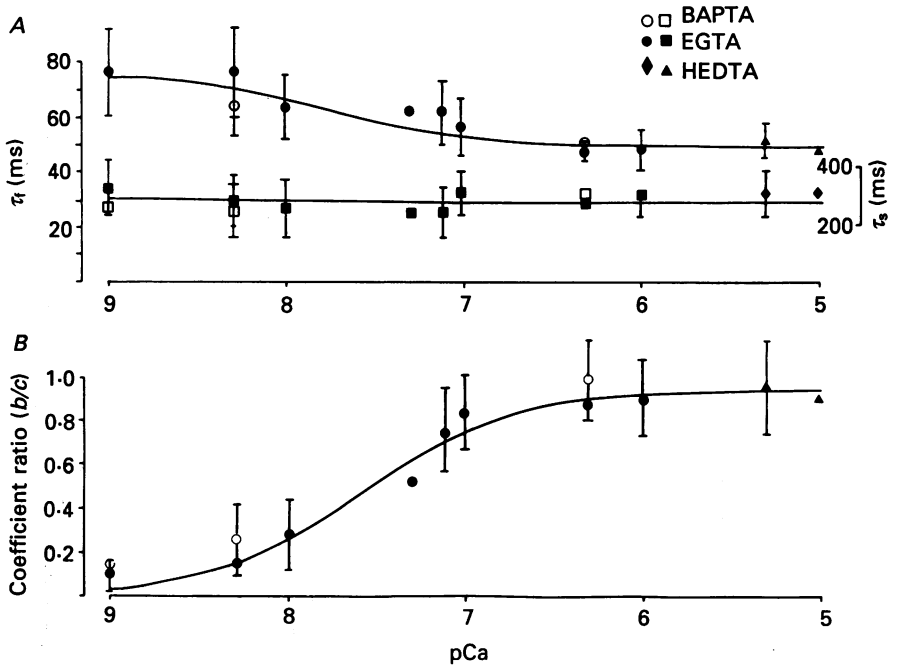

Fig. 8. Relationship between fast (τ_f) and slow (τ_s) time constant of Ca^{2+} inactivation and free [Ca^{2+}] of the internal buffer. *A*, τ_f (upper trace) and τ_s (lower trace) as calculated by a least-squares fitting routine; *B*, ratios (*b*/*c*) of the amplitudes of the fast (*b*) and slow (*c*) inactivation component (for details see Methods) are plotted against the negative logarithm of the free [Ca^{2+}] set by the buffers (pCa). Internal Ca^{2+} chelators were as indicated. Vertical bars indicate standard deviation from the mean ($n = 4$ for the data points). Continuous lines illustrate the predictions obtained from the general reaction scheme described in the Appendix. Temperature 20 °C.

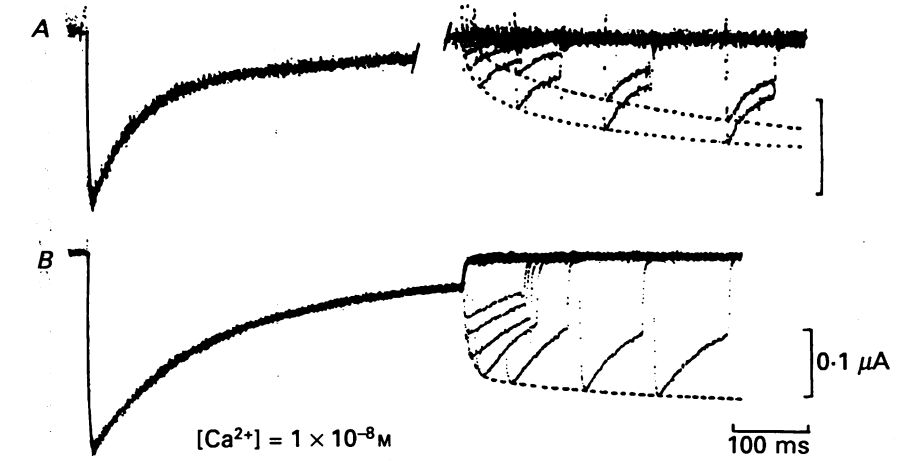

Fig. 9. Recovery from inactivation as a function of free [Ca^{2+}] of the internal buffer. *A*, superimposed current traces during 1 s pre-pulses (only first 0·5 s shown) which were followed by test pulses to +30 mV after repriming pulses of various durations. Envelopes (dashed lines) of the current amplitudes during test pulses indicate the time course of recovery from inactivation for repriming pulses to −50 mV (upper curve) and −130 mV (lower curve) in a cell not pre-loaded with buffer. *B*, as in *A*, for neurone injected with EGTA–Ca^{2+}buffer (free [Ca^{2+}] = 1×10^{-8} M). Pre-pulses were 0·5 s and repriming pulses were to −130 mV. Note that following the injection, recovery was considerably faster and repriming pulses were far more effective. *A* and *B* represent different cells. Temperature 20 °C.

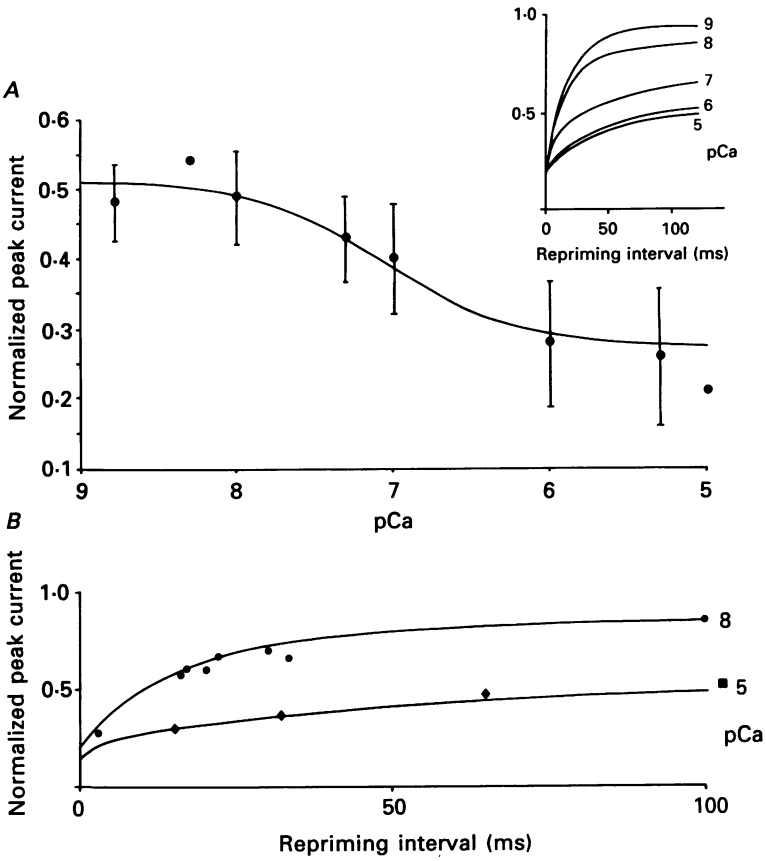

Fig. 10. *A*, relationship between free $[Ca^{2+}]$ of the internal buffer and amount of recovery from inactivation. Depolarizing pulses to +30 mV of 1 s and 400 ms duration, respectively, were separated by 20 ms repriming pulses to −130 mV. Peak current during the second depolarization pulse was normalized to peak current during the pre-pulse and plotted against the negative logarithm of free $[Ca^{2+}]$ set by the buffers (pCa). Vertical bars indicate standard deviation from the mean ($n = 4$ for the data points). Continuous line illustrates the prediction of the general reaction scheme (see Appendix). Inset shows time course of repriming as modelled for various Ca^{2+} concentrations (as indicated). Temperature 20 °C. *B*, same curves as in the inset of *A* for $[Ca^{2+}]$ as indicated. The data points are well fitted by the computer simulations. Inset indicates amount of repriming after 3·75 s for $[Ca^{2+}] = 1 \times 10^{-5}$ M.

relative contribution of the fast time constant was often too small to be detected. The ratio also fell to slightly below one at concentrations greater than 5×10^{-6} M.

Effect of Ca^{2+} buffering on recovery from inactivation

The ability of hyperpolarizing pulses to restore inactivated Ca^{2+} current was greatly enhanced in cells that had been injected with buffers to keep free $[Ca^{2+}]$ at a low level. This is illustrated in Fig. 9 which shows double-pulse experiments in which prolonged pre-pulses to +30 mV were separated from subsequent test pulses of the same magnitude by repolarizing intervals of varied duration. Buffering free $[Ca^{2+}]$ to

1×10^{-8} M increased the effectiveness of repriming considerably, particularly for strongly hyperpolarizing intervals (Fig. 9, Fig. 10*B*). Figure 10*A* summarizes results of double-pulse experiments with 20 ms intervals of hyperpolarization to −130 mV at various levels of free [Ca^{2+}]. The effectiveness of the hyperpolarizing interval increased steeply when [Ca^{2+}] was less than 1×10^{-7} M. Even at buffered [Ca^{2+}] as high as 5×10^{-6} M, the amount of repriming was still greater than that seen with an identical pulse protocol in the same neurones before injection.

DISCUSSION

Characteristics of calcium current inactivation and repriming

The results of the present experiments demonstrate that in these identified molluscan neurones, Ca^{2+} current inactivation depends both on membrane potential and on internal Ca^{2+} concentration. On the one hand, it is evident that the process is not solely voltage-dependent, because replacement of Ca^{2+} by Ba^{2+}, or prevention of intracellular Ca^{2+} accumulation by intracellular injection of Ca^{2+} buffers, alters the time course of inactivation in a systematic fashion and modifies the effectiveness of voltage-dependent repriming. On the other hand, the data demonstrate that the process cannot be solely Ca^{2+}-dependent, either. Thus, we show that the extent of inactivation is not simply related to prior Ca^{2+} entry, and we present direct evidence that repriming is voltage-dependent. Moreover, Ca^{2+} inactivation persisted in cells that were quantitatively injected with Ca^{2+} buffers adjusted to [Ca^{2+}] levels as low as 1×10^{-9} M, while [Ca^{2+}] levels as high as 5×10^{-6} M led to minimal attenuation of the peak current.

That Ca^{2+} inactivation is jointly dependent on membrane potential and internal Ca^{2+} has been concluded for snail neurones (Brown *et al.* 1981; Yatani *et al.* 1983), for heart cells (Kass & Sanguinetti, 1984; Lee *et al.* 1985; Hadley & Hume, 1987; Argibay *et al.* 1988), and for sensory neurones (Akaike *et al.* 1988). In the present experiments, we have used systematic injection of known concentrations of buffered Ca^{2+}, in order to provide a quantitative description of the relationship between internal free [Ca^{2+}] and the parameters of inactivation.

Consequences of spatio-temporal calcium buffering

Findings similar to ours, with internal application of Ca^{2+} chelators, were reported by Brown *et al.* (1981) using internal perfusion techniques, and by Eckert & Ewald (1983) and Plant *et al.* (1983) using injection of EGTA. In the latter two papers, it was suggested that the failure of EGTA to totally suppress Ca^{2+} inactivation reflected insufficient Ca^{2+} buffering at the inner surface of the membrane. We therefore used higher EGTA concentrations than usual, and also applied BAPTA to deal with the amount and speed of anticipated changes in $[Ca^{2+}]_i$ during Ca^{2+} current (for details see Methods).

Considering Ca^{2+} entry through single channels, deviations from the free $[Ca^{2+}]_i$ set by the added buffers occur in a narrow surround of the internal mouth of individual channels. These changes are fast (1–10 μs, see also Neher, 1986) compared to the time course of inactivation and even to observed mean open and short closed times of single channels (about 1 ms, see Lux & Brown, 1984*b*). Hence the spatial

concentration profile which develops during Ca^{2+} influx in the surround of a channel is essentially stationary, and after channel closing the Ca^{2+} concentration at the channel will be quickly reset to the level controlled by the buffer. Since the high concentrations of Ca^{2+} chelators used prevent overlapping of domains of single channels even in 'hot spots', with densities of ten channels per μm^2 (see Methods), a spatial accumulation of Ca^{2+} is not to be expected. We thus focus on local stationary variations in free $[Ca^{2+}]_i$ with the surround of individual channels during random opening and closing. As can be inferred from Fig. 1, buffering to the Ca^{2+} levels set by the BAPTA–Ca^{2+} buffers is already achieved at distances between 10 and 20 nm from the inner channel end, while distances about four times longer apply for EGTA–Ca^{2+} buffers. On the other hand, inactivation does not differ significantly when using BAPTA instead of EGTA (see Fig. 8). These findings strongly suggest that the site which regulates inactivation is located in an area where free $[Ca^{2+}]_i$ is sufficiently controlled by the buffer. This is compatible with the idea that the inactivation substrate is somewhat remote from the channel, or access to it is complicated by diffusional obstacles for Ca^{2+} ions.

An interesting alternative is that a channel, once open, might be insensitive to inactivation. Also in this case inactivation, if coupled to the closed state of the channel, would be basically controlled by the free $[Ca^{2+}]$ of the internal buffer. On the other hand, the assumption that the open channel experiences the high Ca^{2+} concentration at its inner mouth is difficult to reconcile with the high Ca^{2+} sensitivity of inactivation. In this case one would expect that already brief channel openings produce inactivation at maximum rates, even if channel closing by inactivation is not instantaneous. Since there is no experimental evidence for the above-described mechanism (see Lux & Brown, 1984*a*), it seems justified to assume that in our experiments the Ca^{2+} concentration at the site that regulates inactivation is basically determined by the free $[Ca^{2+}]$ set by the buffers.

Model of inactivation

The complex kinetics of Ca^{2+} inactivation can be well modelled on the basis of a Ca^{2+}-dependent process (Standen & Stanfield, 1982; Chad, Eckert & Ewald, 1984). It is, however, obvious from the above that our data cannot be adequately accounted for by such models. We have therefore described inactivation as a Ca^{2+}- and voltage-dependent process with a reaction scheme in which the observed time constants derive from the rates of the transitions between three different states of the Ca^{2+} channel. This approach was chosen since it makes the kinetic system amenable to considerable analysis (Colquhoun & Hawkes, 1983). The data in Fig. 8 give a quantitative picture of how these time constants and the ratio of their coefficients vary as a function of $[Ca^{2+}]_i$. The finding that the two constants are distinct, differing by about a factor of ten under conditions of internal buffering, suggests that there are at least two states of inactivation. We hypothesize that while access to both states is initiated by the voltage step, access to one of them is also controlled by $[Ca^{2+}]_i$.

We assume that inactivation starts from a lumped state of activation (A), without regard to whether the channels are open or closed, and that there are two states of inactivation, IN_V and IN_{Ca}. Only IN_{Ca} is characterized by Ca^{2+}-dependent rates. We

further assume that at membrane potentials of -50 mV and below, there is little steady-state inactivation (the probability of finding the channels in state A at time $t = \infty$, $p_A^\infty = 1$), since increase in the holding potential was without significant effect on the peak Ca^{2+} current. This latter assumption is also consistent with the observation that injection of Ca^{2+} buffers never resulted in an increase in the peak Ca^{2+} current, even with free $[Ca^{2+}]$ below 1×10^{-8} M.

The behaviour of the time constants and of the amplitude ratio b/c (Fig. 8) strongly points to a specific sequence of the three states in order to describe inactivation and recovery. A linear sequence was found sufficient to describe inactivation with varying $[Ca^{2+}]_i$ at a given potential (see Appendix). All effects due to steady-state variation of $[Ca^{2+}]_i$ could be attributed to the transition rate which leads from A to the inactivated state IN_{Ca}. With long depolarizing pulses, a significant occupancy of the inactivated state IN_V is reached, in agreement with previous reports (Kass & Sanguinetti, 1984; Lee *et al.* 1985; Fox, 1981; Hadley & Hume, 1987) which assign the slow component of inactivation to a voltage-dependent process. Ca^{2+} dependence is thus exclusively attributed to IN_{Ca} which rapidly exchanges with state A. The general form of the model provides a transition from IN_V to IN_{Ca}, the rate of which is assumed, for systematic reasons, to be Ca^{2+}-dependent. However, it contributes little to the inactivation process itself (see Appendix).

Recovery from inactivation

On the other hand, this transition was found to be essential to describe recovery from inactivation. The recovered amount of the Ca^{2+} current at a given time increases with hyperpolarization. The time course of recovery becomes particularly fast with low $[Ca^{2+}]_i$, contrary to that of inactivation. This implies an increased efficiency with hyperpolarization of both reaction pathways leading away from the highly occupied state IN_V. With low $[Ca^{2+}]_i$, repriming is due to the direct transition from IN_V to A since IN_{Ca} is hardly available.

With high availability of IN_{Ca}, as in the case of high $[Ca^{2+}]_i$, the transition to IN_{Ca} becomes the dominant one. The return from the now highly occupied state IN_{Ca} to state A is considerably slower than that from IN_V to A. Thus, recovery is dominated by a slow process. Moreover, the steady-state occupancy of state A is reduced under these conditions, because high $[Ca^{2+}]_i$ also facilitates transition from A to IN_{Ca}. In order to deal with slow recovery, the transition from state IN_{Ca} to state A is considered to be weakly, if at all, voltage-dependent (see Appendix).

Particular features of the present model, demanded by the data on Ca^{2+}-dependent recovery, are noteworthy: voltage-dependent inactivation is essentially assigned to the transition between two states which differ by their Ca^{2+}-binding capability (for details see Appendix). The transition between the two inactivation states may be visualized as a conformational change of a protein, where the Ca^{2+}-binding site is particularly voltage-sensitive, which suggests a membrane localization of the substrate for inactivation. The transition rate from state IN_V to state IN_{Ca} at -130 mV is about three to four orders of magnitude larger than that at $+30$ mV. This increase is in line with the view that the ability of one Ca^{2+} ion to bind to its

specific reaction site is essentially determined by the electrochemical driving force.

The general three-state scheme presented appears to be the simplest form for describing the essential features of inactivation and repriming. It is, however, not perceived to account for a slow recovery, which is frequently seen following depolarizing pulses of 1 s or longer in cells which were not injected with Ca^{2+} buffers. Such sustained depolarizations seem to induce long-lasting reactions related to cell Ca^{2+} metabolism (Yatani *et al.* 1983), which are considered to be secondary for the short-term recovery process studied here.

The model as used also appears to be appropriate to describe modulation of the inactivation process.

When Ba^{2+} was the current carrier, inactivation was slowed, and its time course was well-fitted by a single exponential function with a time constant that was slightly smaller than that of the slow component with Ca^{2+} (see Fig. 2). This suggests that the transition to IN_{Ca} is much slower with Ba^{2+} than with Ca^{2+}. Thus, as with Ca^{2+} current under conditions of low $[Ca^{2+}]_i$, repriming of the inactivated Ba^{2+} current is determined by the voltage-dependent transition from IN_V to A, while the alternative pathway to IN_{Ca} is negligible.

It was recently shown that when the cyclic alcohol, menthol, is applied to the outside of the membrane, inactivation and repriming are markedly accelerated in a manner that appears to be independent of changes in $[Ca^{2+}]_i$ (Swandulla, Schäfer & Lux, 1986; Swandulla, Carbone, Schäfer & Lux, 1987). The effect on inactivation may be explained in the framework of our model if we assume that in the presence of menthol, the usually Ca^{2+}-dependent transitions to state IN_{Ca} are as fast as or even faster than in the presence of high $[Ca^{2+}]_i$. In this case, voltage dependence of the transition from IN_{Ca} to A becomes essential to describe recovery from inactivation.

Functional implications

Joint regulation by internal Ca^{2+} and membrane potential of Ca^{2+} channel inactivation and recovery may be important for determining the activities of neurones with prominent Ca^{2+} conductance. Our data indicate that even under conditions of relatively high, sustained $[Ca^{2+}]_i$, voltage-dependent Ca^{2+} channels will not necessarily become unavailable for activation. In most neurones, Ca^{2+} influx triggers a Ca^{2+}-dependent K^+ current, which results in hyperpolarization. Findings such as those illustrated in Fig. 5*A* indicate that by including voltage-dependent repriming of inactivated channels, even short-lasting after-hyperpolarizations could foster prolongation of Ca^{2+}-dependent activities despite considerable intracellular Ca^{2+} accumulation.

APPENDIX

Three-state model of Ca^{2+} inactivation

The time course of inactivation shows two clearly distinguishable time constants, and requires at least a three-state reaction scheme to describe the inactivation process (Colquhoun & Hawkes, 1977). Our approach considers a circular three-state

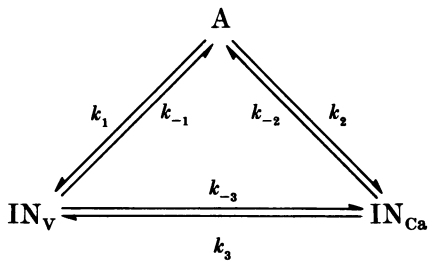

(M1)

reaction scheme (M1) of Ca^{2+} channel states. Other possible schemes are discussed and evaluated in a separate section.

The formalism used for the mathematical treatment of (M1) is as described by Colquhoun & Hawkes (1977) for a Markov process with discrete states in continuous time. The basic expressions that define the system are given below (IN_V and IN_{Ca} are abbreviated as V and Ca in the subscripts of the following equations):

(1) In equilibrium the probabilities p_A^∞, p_{Ca}^∞ and p_V^∞ of the system being in the state A, IN_{Ca} and IN_V respectively are calculated (see King & Altman, 1956) using:

$$p_A^\infty = S_A/S_D; \quad p_{Ca}^\infty = S_{Ca}/S_D; \quad p_V^\infty = S_V/S_D, \tag{1}$$

with

$$S_A = k_{-1}k_{-2} + k_{-1}k_3 + k_{-2}k_{-3}, \tag{2}$$

$$S_{Ca} = k_2k_{-3} + k_2k_{-1} + k_1k_{-3}, \tag{3}$$

$$S_V = k_1k_3 + k_1k_{-2} + k_2k_3, \tag{4}$$

$$S_D = S_A + S_{Ca} + S_V, \tag{5}$$

where k_i ($i = 1, 2, 3, -1, -2, -3$) are the transition rates of (M1).

(2) In non-equilibrium the probability of finding the system in one of the states at time t follows the sum of two exponential terms. For $p_A(t)$, which describes the time course of the measured Ca^{2+} currents, the explicit expression is:

$$p_A(t) = p_A^\infty + b\exp(-\lambda_1 t) + c\exp(-\lambda_2 t). \tag{6}$$

The parameters are given by:

$$b = [\lambda_2(p_A^\infty - p_A^0) + p_A^0(k_1 + k_2) - k_{-1}p_V^0 - k_{-2}p_{Ca}^0]/(\lambda_1 - \lambda_2), \tag{7}$$

$$c = [\lambda_1(p_A^\infty - p_A^0) + p_A^0(k_1 + k_2) - k_{-1}p_V^0 - k_{-2}p_{Ca}^0]/(\lambda_2 - \lambda_1), \tag{8}$$

$$\lambda_1 = \tfrac{1}{2}\Sigma k_i + [\tfrac{1}{4}(\Sigma k_i)^2 - S_D]^{\frac{1}{2}} \quad (i = 1, 2, 3, -1, -2, -3), \tag{9}$$

$$\lambda_2 = \tfrac{1}{2}\Sigma k_i - [\tfrac{1}{4}(\Sigma k_i)^2 - S_D]^{\frac{1}{2}} \tag{10}$$

and

$$\lambda_1\lambda_2 = S_D, \tag{11}$$

where b and c represent the weighting factors, λ_1 and λ_2 the reciprocals of the time constants of the reactions towards equilibrium, and p^0 and p^∞ the occupational probabilities of the indicated states at time $t = 0$ and ∞, respectively.

Calcium inactivation modelled as a calcium- and voltage-dependent process

In our model, state A is the conducting state of the Ca^{2+} channel, which includes silent but not inactivated substates whose transitions to conducting states are rapid

compared to those of the model. We have assumed that inactivation starts from this lumped state of activation since there is no direct evidence that inactivation is attained from a particular state (see Brown, Lux & Wilson, 1984; Lux & Brown, 1984*a*; Chad & Eckert, 1986).

The probability of finding the channel in state IN_{Ca} depends on the internal Ca^{2+} concentration. We assume that IN_{Ca} can be reached only if Ca^{2+} can react with a site R at or near the channel so that the probability p for a Ca^{2+} ion being bound to R is

$$p = (1+K_D/[Ca^{2+}]_i)^{-1}, \tag{12}$$

where $[Ca^{2+}]_i$ is the free internal Ca^{2+} concentration and K_D is the dissociation constant. The rates of the transitions leading to IN_{Ca} are then given by:

$$k_2 = k_2^* p, \tag{13}$$

and

$$k_{-3} = k_{-3}^* p, \tag{14}$$

where k_2^* and k_{-3}^* are the maximal possible transition rates.

To describe both inactivation and recovery from inactivation adequately at least two rates have to be voltage-dependent. Recovery during hyperpolarization shows a component that is fast ($\lambda_1 = 50\ s^{-1}$) compared to that during depolarization, but with higher $[Ca^{2+}]_i$ a slow process becomes dominant (Fig. 9). At least a tenfold decrease of the weighting factor b in eqn (6) is necessary to describe the change of the recovery kinetics with increasing $[Ca^{2+}]_i$ between 10^{-9} and 10^{-5} M as shown in Fig. 10. This is only attributable to the increase of λ_1 with $[Ca^{2+}]_i$ since the other terms in eqn (7) are either Ca^{2+}-independent or produce an increase of b with $[Ca^{2+}]_i$. With these restrictions given by the experimental data it follows from eqns (9), (10) and (11) that k_{-1} and k_{-3}^* have to be the voltage-dependent rates.

Computer simulations

The above-defined qualities of the reaction scheme were used to predict the time course of the inactivation and recovery process estimating the rates with a gradient-expansion algorithm (Marquardt, 1963).

For inactivation, in accordance with the observation that neither variation in free $[Ca^{2+}]_i$ nor holding potentials negative to -50 mV affect peak inward currents significantly, the probability of the channels at time $t = 0$ (p_A^0) being in state A is assumed to be one. Consequently p_V^0 and p_{Ca}^0 are zero. Thus, using eqns (7) and (8),

$$b/c = -[\lambda_2(p_A^\infty - 1) + k_1 + k_2]/[\lambda_1(p_A^\infty - 1) + k_1 + k_2]. \tag{15}$$

Ratios b/c (Fig. 8) were fitted with all rates allowed to vary freely. The rates obtained in this manner also gave a good estimate of λ_1 and λ_2 (see continuous lines in Fig. 8). The estimated rates are (in s^{-1}): $k_1 = 2{\cdot}57$; $k_2^* = 7{\cdot}47$; $k_3 = 2{\cdot}77$; $k_{-1} = 0{\cdot}68$; $k_{-2} = 10{\cdot}02$; $k_{-3}^* = 0{\cdot}08$.

To describe recovery from inactivation eqns (6) to (10) were used. Occupational probabilities of the states at the end of the depolarizing pulse were introduced as the initial values p_A^0, p_V^0, p_{Ca}^0. To fit the time course of recovery, the voltage-dependent rates k_{-3}^* and k_{-1} were allowed to vary while the other rates were as used for inactivation. The estimated values are (in s^{-1}): $k_{-3}^* = 358{\cdot}0$ and $k_{-1} = 50{\cdot}2$.

The scheme describes well the time course of the recovery process during the first

seconds, despite the fact that incomplete recovery is generated with p_A^∞ between 0·94 and 0·55 for $[Ca^{2+}]_i$ varying between 10^{-9} and 10^{-6} M. The actual final attainment of a constant state A with $p_A^\infty = 1$ suggests an additional recovery process. Since this process requires tens of seconds to minutes, it was not considered in the reaction scheme (see Discussion).

Linear three-state reaction schemes

The reaction schemes considered are:

$$IN_V \underset{k_1}{\overset{k_{-1}}{\rightleftharpoons}} A \underset{k_{-2}}{\overset{k_2}{\rightleftharpoons}} IN_{Ca}, \tag{M2}$$

$$IN_V \underset{k_3}{\overset{k_{-3}}{\rightleftharpoons}} IN_{Ca} \underset{k_2}{\overset{k_{-2}}{\rightleftharpoons}} A, \tag{M3}$$

$$IN_{Ca} \underset{k_{-3}}{\overset{k_3}{\rightleftharpoons}} IN_V \underset{k_1}{\overset{k_{-1}}{\rightleftharpoons}} A. \tag{M4}$$

As shown in Fig. 8, the slow time constant of the inactivation process τ_s and thus λ_2 are not particularly Ca^{2+}-dependent. For simplicity we therefore assumed a constant λ_2 to derive the conditions for each reaction scheme using the above equations.

For (M3), λ_2 is constant only if it is identical to zero, while for (M4) a constant λ_2 results in a decrease of the ratio b/c with increased $[Ca^{2+}]_i$. Both conditions are in contrast to the experimental data (see Fig. 8), thus (M3) and (M4) are excluded.

The analogue treatment for scheme (M2) produces an acceptable linear model to describe inactivation under the constraint $k_{-1} = k_{-2}$. For the adopted model (M1), the conditions derived for a constant λ_2 are $k_1 = k_3$ and $k^*_{-3} = 0$, which are well approximated by the rates generated by fitting the inactivation time course (see above). Scheme (M2), however, cannot describe recovery from inactivation since the transition from IN_V to IN_{Ca} which is essential for this process is not represented in this reaction scheme.

This work was supported in part by a grant from the Minerva Foundation to Dr M. J. Gutnick.

REFERENCES

ADAMS, D. J. & GAGE, P. W. (1980). Divalent ion current and the delayed potassium conductance in an *Aplysia* neurone. *Journal of Physiology* **304**, 297–313.

AKAIKE, N., TSUDA, Y. & OYAMA, Y. (1988). Separation of current- and voltage-dependent inactivation of calcium current in frog sensory neuron. *Neuroscience Letters* **84**, 46–50.

ARGIBAY, J. A., FISCHMEISTER, R. & HARTZELL, C. H. (1988). Inactivation, reactivation and pacing dependence of calcium current in frog cardiocytes: correlation with current density. *Journal of Physiology* **401**, 201–226.

ARMSTRONG, C. M. & MATTESON, D. R. (1985). Two distinct populations of calcium channels in a clonal line of pituitary cell. *Science* **227**, 65–67.

ASHCROFT, F. M. & STANFIELD, P. R. (1981). Calcium dependence of the inactivation of calcium currents in skeletal muscle fibers of an insect. *Science* **213**, 224–226.

BEAN, B. P. (1985). Two kinds of calcium channels in canine atrial cells. *Journal of General Physiology* **86**, 1–31.

BOSSU, J. L., FELTZ, A. & THOMANN, J. M. (1985). Depolarization elicits two distinct calcium currents in vertebrate sensory neurons. *Pflügers Archiv* **403**, 360–368.

BREHM, E. & ECKERT, R. (1978). Calcium entry leads to inactivation of calcium current in *Paramecium*. *Science* **202**, 1203–1206.

BREHM, E., ECKERT, R. & TILLOTSON, D. (1980). Calcium-mediated inactivation of calcium current in *Paramecium*. *Journal of Physiology* **306**, 193–203.

BROWN, A. M., LUX, H. D. & WILSON, D. L. (1984). Activation and inactivation of single calcium channels in snail neurons. *Journal of General Physiology* **83**, 751–769.

BROWN, A. M., MORIMOTO, K., TSUDA, Y. & WILSON, D. L. (1981). Calcium current-dependent and voltage-dependent inactivation of calcium channels in *Helix aspera*. *Journal of Physiology* **320**, 193–218.

CARBONE, E. & LUX, H. D. (1984). A low voltage-activated calcium conductance in embryonic chick sensory neurons. *Biophysical Journal* **46**, 413–418.

CHAD, J. E. & ECKERT, R. (1984). Calcium 'domains' associated with individual channels may account for anomalous voltage relations of Ca-dependent responses. *Biophysical Journal* **45**, 993–999.

CHAD, J. E. & ECKERT, R. (1986). An enzymatic mechanism for calcium current inactivation in dialysed *Helix* neurones. *Journal of Physiology* **378**, 31–51.

CHAD, J. E., ECKERT, R. & EWALD, D. (1984). Kinetics of calcium-dependent inactivation of calcium current in voltage-clamped neurones of *Aplysia californica*. *Journal of Physiology* **347**, 279–300.

COLQUHOUN, D. & HAWKES, A. G. (1977). Relaxation and fluctuations of membrane currents that flow through drug-operated ion channel. *Proceedings of the Royal Society B* **199**, 231–262.

COLQUHOUN, D. & HAWKES, A. G. (1983). The principles of the stochastic interpretation of ion-channel mechanisms. In *Single-channel Recording*, ed. SAKMANN, B. & NEHER, E., pp. 135–175. New York: Plenum Press.

CONNOR, J. A. (1979). Calcium current in molluscan neurones: measurement under conditions which maximize its visibility. *Journal of Physiology* **286**, 41–60.

CONNOR, J. A. & NIKOLAKOPOULOU, N. (1982). Calcium diffusion and buffering in nerve cytoplasm. *Lectures on Mathematics in the Life Sciences* **15**, 79–101.

CRANK, J. (1956). *The Mathematics of Diffusion*. Oxford: Clarendon.

DEITMER, J. W. (1984). Evidence for two voltage-dependent calcium currents in the membrane of the ciliate *Stylonychia*. *Journal of Physiology* **355**, 137–158.

ECKERT, R. & CHAD, J. E. (1984). Inactivation of Ca channels. *Progress in Biophysics and Molecular Biology* **44**, 215–267.

ECKERT, R. & EWALD, D. (1983). Inactivation of Ca conductance characterized by tail current measurements in neurones of *Aplysia californica*. *Journal of Physiology* **345**, 549–565.

ECKERT, R. & TILLOTSON, D. (1981). Calcium-mediated inactivation of the calcium coductance in caesium-loaded giant neurones of *Aplysia californica*. *Journal of Physiology* **314**, 265–280.

FEDULOVA, S. A., KOSTYUK, P. G. & VESELOVSKY, N. S. (1985). Two types of calcium channels in the somatic membrane of new-born rat dorsal root ganglion neurones. *Journal of Physiology* **359**, 431–446.

FOX, A. P. (1981). Voltage-dependent inactivation of a calcium channel. *Proceedings of the National Academy of Sciences of the USA* **80**, 2240–2242.

HADLEY, R. W. & HUME, J. R. (1987). An intrinsic potential-dependent inactivation mechanism associated with calcium channels in guinea-pig myocytes. *Journal of Physiology* **389**, 205–222.

HAGIWARA, S. & BYERLY, L. (1981). Calcium channel. *Annual Review of Neuroscience* **4**, 69–125.

HARAFUJI, H. & OGAWA, Y. (1980). Re-examination of the apparent binding constant of ethylene glycol bis (β-aminoethyl ether)-*N,N,N',N'*-tetra-acetic acid with calcium around neutral pH. *Journal of Biochemistry* **87**, 1305–1312.

HOFMEIER, G. & LUX, H. D. (1981). The time courses of intracellular free calcium and related electrical effects after injection of $CaCl_2$ into neurons of the snail, *Helix pomatia*. *Pflügers Archiv* **391**, 242–251.

KASS, R. S. & SANGUINETTI, M. C. (1984). Inactivation of calcium channel current in the calf cardiac Purkinje fiber. *Journal of General Physiology* **84**, 705–726.

KING, E. L. & ALTMAN, C. (1956). A schematic method of deriving the rate laws for enzyme-catalyzed reactions. *Journal of Physical Chemistry* **60**, 1375–1378.

KOSTYUK, P. G. (1980). Calcium ionic channels in electrically excitable membrane. *Neuroscience* **5**, 945–959.

KOSTYUK, P. G. & KRISHTAL, O. A. (1977). Separation of sodium and calcium currents in the somatic membrane of mollusc neurones. *Journal of Physiology* **270**, 545–568.

LEE, K. S., MARBAN, E. & TSIEN, H. W. (1985). Inactivation of calcium channels in mammalian heart cells: joint dependence on membrane potential and intracellular calcium. *Journal of Physiology* **364**, 395–411.

LUX, H. D. & BROWN, A. M. (1984*a*). Single channel studies on Ca inactivation of calcium currents. *Science* **225**, 432–434.

LUX, H. D. & BROWN, A. M. (1984*b*). Patch and whole cell calcium currents recorded simultaneously in snail neurons. *Journal of General Physiology* **83**, 727–750.

LUX, H. D. & GUTNICK, M. J. (1986). Voltage-dependent repriming of inactivated calcium current in identified *Helix* neurons. *Experimental Brain Research* **S14**, 51–60.

LUX, H. D. & HOFMEIER, G. (1982). Properties of a calcium- and voltage-activated potassium current in *Helix pomatia* neurons. *Pflügers Archiv* **394**, 61–69.

MAGURA, I. S. (1977). Long lasting inward current in snail neurons in barium solutions in voltage-clamp conditions. *Journal of Membrane Biology* **35**, 239–256.

MARQUARDT, D. W. (1963). An algorithm for least-squares estimation of nonlinear parameters. *Journal of the Society for Industrial and Applied Mathematics* **11**, 431–441.

MARTELL, A. & SMITH, R. M. (1974). *Critical Stability Constants*, vol. I. New York: Plenum Press.

NEHER, E. (1986). Concentration profiles of intracellular calcium in the presence of a diffusible chelator. *Experimental Brain Research* S14, 80–96.

NOWYCKY, M. C., FOX, A. P. & TSIEN, R. W. (1985). Three types of neuronal calcium channel with different calcium agonist sensitivity. *Nature* **316**, 440–443.

PLANT, T. D. & STANDEN, N. B. (1981). Calcium current inactivation in identified neurones of *Helix aspersa*. *Journal of Physiology* **321**, 273–285.

PLANT, T. D., STANDEN, N. B. & WARD, T. A. (1983). The effects of injection of calcium ions and calcium chelators on calcium channel inactivation in *Helix* neurones. *Journal of Physiology* **334**, 189–212.

QUAST, U., LABHARDT, A. M. & DOYLE, V. M. (1984). Stopped-flow kinetics of the interaction of the fluorescent calcium indicator Quin 2 with calcium ions. *Biochemical and Biophysical Research Communications* **123**, 604–611.

STANDEN, N. B. & STANFIELD, P. R. (1982). A binding site model for calcium channel inactivation that depends on calcium entry. *Proceedings of the Royal Society* B **217**, 101–110.

SWANDULLA, D., CARBONE, E., SCHÄFER, K. & LUX, H. D. (1987). Effect of menthol on two types of Ca currents in cultured sensory neurons of vertebrates. *Pflügers Archiv* **409**, 52–59.

SWANDULLA, D., LUX, H. D., GUTNICK, M. J. & ZUCKER, H. (1988). Joint dependence of calcium channel inactivation on voltage and intracellular calcium in snail neurons. *Journal of General Physiology* **92**, 5a (abstract).

SWANDULLA, D., SCHÄFER, K. & LUX, H. D. (1986). Calcium channel current inactivation is selectively modulated by menthol. *Neuroscience Letters* **68**, 23–28.

THOMPSON, S. & COOMBS, J. (1988). Spatial distribution of Ca currents in molluscan neuron cell bodies and regional differences in the strength of inactivation. *Journal of Neuroscience* **8**, 1929–1939.

TILLOTSON, D. (1979). Inactivation of Ca conductance dependent on entry of Ca ions in molluscan neurons. *Proceedings of the National Academy of Sciences of the USA* **76**, 1497–1500.

TSIEN, R. W. (1983). Calcium channels in excitable membranes. *Annual Review of Physiology* **45**, 341–358.

TSIEN, R. Y. (1980). New calcium indicators and buffers with high selectivity against magnesium and protons: design, synthesis, and properties of prototype structures. *Biochemistry* **19**, 2396–2404.

YATANI, A., WILSON. D. L. & BROWN, A. M. (1983). Recovery of Ca currents from inactivation: the roles of Ca influx, membrane potential, and cellular metabolism. *Cellular and Molecular Neurobiology* **314**, 381–395.

ZUCKER, R. S. (1981). Tetraethylammonium contains an impurity which alkalizes cytoplasm and reduces calcium buffering in neurons. *Brain Research* **208**, 473–478.